New Spectrophotometer System for Measuring Thermal Radiation Characteristics of Real Surfaces of Thermal Engineering Entirely

AUTHOR(S):

MAKINO, Toshiro; WAKABAYASHI, Hidenobu

CITATION:

MAKINO, Toshiro ...[et al]. New Spectrophotometer System for Measuring Thermal Radiation Characteristics of Real Surfaces of Thermal Engineering Entirely. Journal of Thermal Science and Technology 2011, 6(1): 80-92

ISSUE DATE:

2011-03-22

URL:

http://hdl.handle.net/2433/197340

Journal of Template
Vol. 00, No. 0, 0000

New Spectrophotometer System for Measuring Thermal Radiation Characteristics of Real Surfaces of Thermal Engineering Entirely*

Toshiro MAKINO and Hidenobu WAKABAYASHI
Department of Mechanical Engineering and Science, Kyoto University,
Kyoto 606-8501, Japan
E-mail: makino.toshiro.2a@kyoto-u.ac.jp

Abstract

In this work we develop a new spectrophotometer system for measuring thermal radiation characteristics of real surfaces of thermal engineering. This system measures transition of spectra of normal incidence hemispherical reflectance R_{NH}, normal incidence specular reflectance R_{NN}, normal incidence diffuse reflectance R_{ND}, normal incidence absorptance A_N and normal emittance ε_N of real surfaces in a near-ultraviolet through infrared region of wavelength 0.30~10.9 μm simultaneously and repeatedly with a cycle time of 6 s. The system is applied to measure the spectrum transition of the reflectances, absorptance and emittance of a nickel surface which is prepared as a clean optically smooth surface and is oxidized in high-temperature air to be changed to an oxidized rough real surface. Microscopic mechanisms of the spectrum transition are discussed, to illustrate the performance of the developed spectrophotometer system for thermal engineering applications.

Key words: Thermal Radiation, Spectroscopic Measurement, Simultaneous Measurement, Reflectance, Absorptance, Emittance, Real Surface

1. Introduction

Thermal radiation characteristics of surfaces are one of the most important subjects of fundamental research in thermal engineering. Surfaces of thermal engineering are real surfaces in natural and/or industrial environments, and the surfaces reflect radiation more or less diffusely. The surface microstructure changes at every moment in the crude environment, or the surface microstructure is changed actively in the surface micro-fabrication processes.

In order to investigate the reflection, absorption and emission characteristics of such real surfaces, an individual measurement system should be developed for thermal engineering[1, 2]. The points of the development of the measurement system are summarized as follows. (1) The characteristics should be investigated spectrally in a wide spectral region from visible through infrared to which Planck distribution extends. (2) Knowledge of directional characteristics of radiation is important, and the measurement system should be able to evaluate the hemispherical reflection, specular reflection and diffuse deflection separately. (3) The measurement system should also be able to follow the transition of radiation characteristics with the change of the surface microstructure at the real time.

In 2001 the authors developed a spectrophotometer system for measuring the transition of spectra of normal incidence specular reflectance R_{NN} and normal emittance ε_N in a near-ultraviolet through infrared region simultaneously and repeatedly[3]. This system

*Received XX Xxx, 200X (No. XX-XXXX)
[DOI: 00.0000/ABCDE.2006.000000]

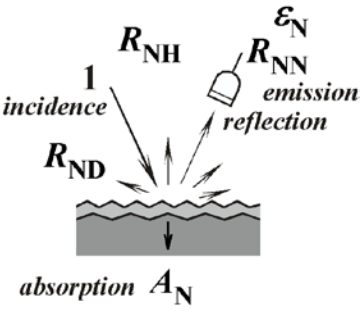

Figure 1. Concepts of normal incidence hemispherical reflectance R_{NH}, normal incidence specular reflectance R_{NN}, normal incidence diffuse reflectance R_{ND}, normal incidence absorptance A_N and normal emittance ε_N.

clarified the dynamics of transition of radiation characteristics of real surfaces of metals, and enabled us to diagnose the change of temperature and microstructure of the surface at the real time[4]. The experimental work with the system suggested a possibility of the development of a spectrally-functional surface for the TPV emitter[5]. The authors also developed another spectrophotometer system for measuring the spectra of normal incidence hemispherical reflectance R_{NH} and normal emittance ε_N simultaneously and repeatedly[6] on the basis of the former system[3]. The new system measured rigorously defined hemispherical reflectance R_{NH} and it enabled us to evaluate the spectra of normal incidence absorptance A_N. The authors employed this system to examine Kirchhoff's law on thermal radiation[7], and also employed it to find a new radiation phenomenon of high temperature palladium[8].

In order to clarify radiation characteristics in thermal engineering entirely, further development of the spectrophotometer system is desirable. That is, transition of the spectra of such quantities as shown in Figure 1 should be readily measured in a wide spectral region simultaneously and repeatedly. The quantities in the figure are normal incidence hemispherical reflectance R_{NH}, normal incidence specular reflectance R_{NN}, normal incidence diffuse reflectance R_{ND}, normal incidence absorptance A_N and normal emittance ε_N. In the figure "normal" is drawn in a near-normal direction.

In the present work, we develop a new spectrophotometer system which measures the transition of spectra of radiation quantities as shown in Figure 1 entirely in a near-ultraviolet through infrared region on the basis of the previous spectrophotometer system [3, 6]. The spectrum transition from a clean optically smooth nickel surface to an oxidized rough surface in a high-temperature air-oxidation process is measured to demonstrate the performance of the developed spectrophotometer system.

Nomenclature

A_N : normal incidence absorptance
d : thickness of surface film, m
n : index of refraction
R_{HN} : normal reflectance for hemispherically homogeneous incidence
R_{ND} : normal incidence diffuse reflectance, diffuse reflection component of R_{NH}
R_{NH} : normal incidence hemispherical reflectance
R_{NN} : normal incidence specular reflectance, specular reflection component of R_{NH}
t : time after the start of surface heating, s
ε_N : normal emittance
λ : wavelength of radiation in vacuum, m

$\lambda_{(1)}$: wavelength of valley of oscillation of the 1st-order interference in spectrum of reflectance R_{NN}
σ : rms roughness of surface, m

Subscripts

B : blackbody
H : hemispherically homogeneous incidence, hemispherical reflection
N : normal, 15°-direction incidence, reflection and emission in experiment

2. Experimental System and Procedure

2.1 Ideas for spectrophotometer system

Of the radiation quantities of reflection, absorption and emission as shown in Figure 1, normal incidence hemispherical reflectance R_{NH} is one of the most important quantities to be measured. From the point of view of designing the experimental system, however, direct measurement of normal incidence hemispherical reflectance R_{NH} is not easy, but the measurement of normal reflectance R_{HN} for hemispherically homogeneous incidence is preferable. Since Helmholtz reciprocal law[9],

$$R_{NH}=R_{HN} \tag{1}$$

holds, normal incidence hemispherical reflectance R_{NH} is obtained by the measurement of R_{HN}. Additionally when normal incidence specular reflectance R_{NN}, specular reflection component of hemispherical reflectance R_{NH} is measured simultaneously, then normal incidence diffuse reflectance R_{ND}, diffuse component of hemispherical reflectance R_{NH} is obtained by,

$$R_{ND}=R_{NH}-R_{NN} \tag{2}$$

simultaneously, and normal incidence absorptanceA_N is obtained by,

$$A_N=1-R_{NH} \tag{3}$$

simultaneously.

We develop a spectrophotometer system for measuring the spectra of normal reflectance R_{HN} for hemispherically homogeneous incidence, normal incidence specular reflectance R_{NN} and normal emittance ε_N simultaneously and repeatedly. Since the measurement of “normal incidence specular reflection” is not easy, “normal” is substituted actually by the measurement for incident angle, reflection angle and emission angle of 15°.

2.2 Spectrophotometer system

Figure 2 shows a sketch of the optical sub-system for measuring normal reflectance R_{HN} for hemispherically homogeneous incidence, normal incidence specular reflectance R_{NN} and normal emittance ε_N developed in this work. This optical sub-system is connected to the previously developed spectrophotometer system[3, 6]. Figure 3 shows the schematic diagram of the new spectrophotometer system with the new optical sub-system.

In Figures 2 and 3 two paraboloidal mirrors /3/ and /4/ of 120 mm in diameter are set facing to each other. The two paraboloidal mirrors have holes of 12 mm in diameter in the central parts. A tungsten-halogen lamp /1/ for near-ultraviolet through near-infrared region or a silicon nitride light source /2/ for infrared region is set at the focal point of the paraboloidal mirror /3/. The sizes of the light sources /1/ and /2/ are 3.3×0.6 mm and

4.7×1.3 mm, respectively. These light sources emit radiation whose intensity is approximately isotropic.

The two light sources are alternatively set at the focal point of the paraboloidal mirror /3/ or at an off-focal point by the help of a cam mechanics /0/ (in Figure 3) driven by a computer-controlled stepping motor. When one of the two light sources is set at the focal point diffusely emitted radiation is transformed to a parallel flux by the paraboloidal mirror /3/ to proceed to another paraboloidal mirror /4/. A specimen /5/ is set at the focal point of the paraboloidal mirror /4/. The surface of the specimen /5/ is inclined by 15° from the optical axis of the paraboloidal mirror /4/. On the surface of the specimen /5/ radiation whose intensity is hemispherically homogeneous is incident from the paraboloidal mirror /4/ and focuses. A component of the hemispherically reflected radiation which proceeds in the direction of 15°-reflection is led through a hole on the paraboloidal mirror /4/ to the spectrometer and detector sub-systems and measured. The 15°-reflection is assumed to be normal reflection and the measured component is assumed to be the normal reflection component for hemispherically homogeneous incidence. With respect to the spectrometer and detector sub-systems of the spectrophotometer system Reference (3) describes in detail.

In order to measure the 15°-incidence specular reflection, which is assumed to be normal incidence specular reflection, a shutter disk /7/ of 130 mm in diameter is inserted and removed in the optical path between the two paraboloidal mirrors /3/ and /4/. The disk /7/ has a hole of 13 mm in diameter at the position of 16 mm from the center of the disk. When the disk /7/ does not interrupt the parallel flux, the hemispherically homogeneous radiation is incident on the surface of the specimen /5/. When the disk /7/ interrupts the parallel flux a portion of the flux which comes through the hole on the disk is incident on the surface of the specimen /5/ from the 15°-direction. In the latter case, the component reflected on the surface of the specimen /5/ in the specular direction, which is assumed to the normal incidence specular reflection component, is led to the spectrometer and detector sub-systems and measured.

From the surface of the specimen /5/, besides the above-mentioned reflection components, radiation component emitted by the surface itself in the direction of emission angle of 15°, which is assumed to be normal emission, is led through the hole of the paraboloidal mirror /4/ to the spectrometer and detector sub-systems and measured. That is, <reflection + emission> is measured. On the other hand, when both of the light sources /1/ and /2/ are set at off-focal points radiation is not incident on the specimen surface and only

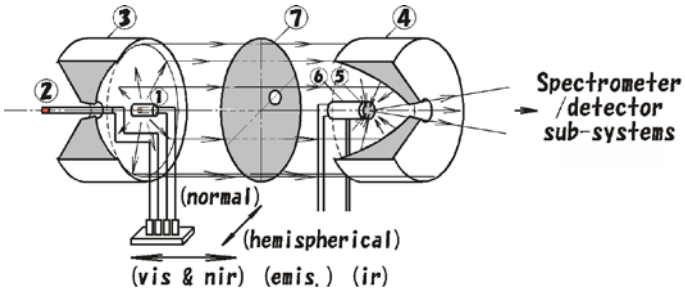

1. tungsten-halogen lamp
2. Si_3N_4 light source
3. paraboloidal mirror 1
4. paraboloidal mirror 2
5. specimen
6. heater
7. shutter disk

Figure 2. Sketch of optical sub-system for measuring normal reflectance R_{HN} for hemispherically homogeneous incidence, normal incidence specular reflectance R_{NN} and normal emittance ε_N.

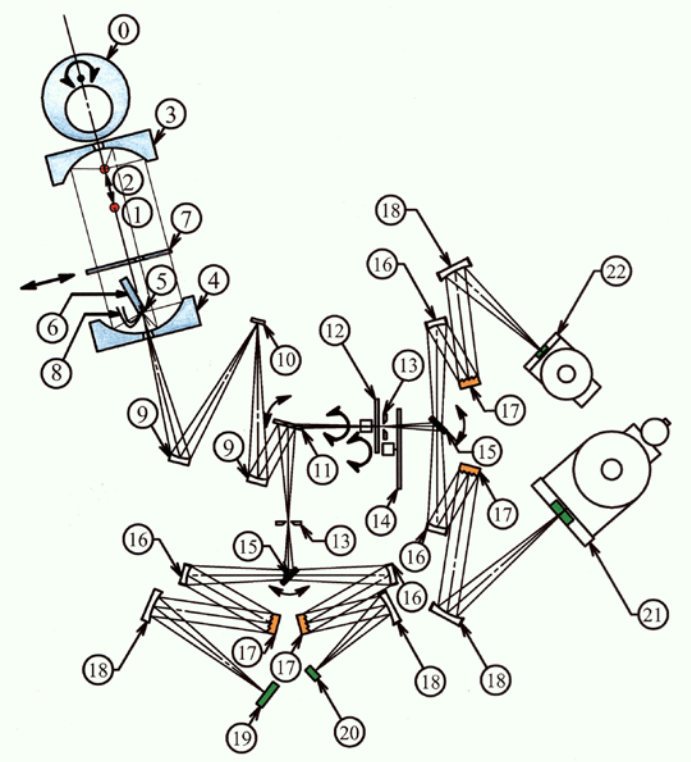

0. cam mechanics
1. tungsten-halogen lamp
2. Si_3N_4 light source
3. paraboloidal mirror 1
4. paraboloidal mirror 2
5. specimen
6. heater
7. shutter disk
8. thermocouple
9. concave mirror
10. plane mirror
11. rotational plane mirror
12. optical chopper
13. entrance slit
14. filter disk
15. rotational plane mirror
16. collimator
17. diffraction grating
18. camera mirror
19. 35-Si photodiode array
20. 16-Ge photodiode array
21. 32-InSb photovoltaic detector array
22. 16-HgCdTe photoconductive detector array

Figure 3. Schematic diagram of wide-spectral-range high-speed spectrophotometer system for measuring spectra of normal reflectance R_{HN} for hemispherically homogeneous incidence, normal incidence specular reflectance R_{NN} and normal emittance ε_N.

<emission> of the specimen surface is measured. From these measured values, the normal reflection component for hemispherically homogeneous incidence, normal incidence specular reflection component and the emission component are separated readily.

In the spectral measurement, reflection spectra of 93 wavelength points of λ=0.30~10.9 μm and emission spectra of 42 wavelength points of λ=1.93~10.9 μm are measured simultaneously and repeatedly with a cycle time of 6 s. Absolute values of normal reflectance R_{HN} for hemispherically homogeneous incidence and normal incidence specular reflectance R_{NN} are determined on the basis of a specular reflection spectrum measured on a clean optically smooth nickel surface and a published spectra of the optical constants[10]. Absolute values of normal emittance ε_N are determined on the basis of normal emission

spectra measured on a blackbody[6] whose apparent normal emittance is 0.99. Measured spectra of normal reflectance R_{HN} for hemispherically homogeneous incidence, normal incidence specular reflectance R_{NN} and normal emittance ε_N are interpreted by Equations (1)~(3) to those of normal incidence hemispherical reflectance R_{NH}, normal incidence diffuse reflectance R_{ND} and normal incidence absorptance A_N.

In the following sections we call for simplicity the normal incidence hemispherical reflectance R_{NH}, normal incidence specular reflectance R_{NN} and normal incidence diffuse reflectance R_{ND} as hemispherical reflectance, specular reflectance and diffuse reflectance, respectively, and the normal incidence absorptance A_N and normal emittance ε_N as absorptance and emittance, respectively.

2.3 Experimental procedure

Material of the specimen is a polycrystalline nickel plate of 99.9 % in purity. The plate is fabricated to be a disk of 10.5 mm in diameter and 1 mm in thickness, and the surface is buffed to realize an optically smoothness of the maximum roughness less than 30 nm. The finished surface reflects visible radiation specularly. We measure the transition of the spectra of normal reflectance R_{HN} for hemispherically homogeneous incidence, specular reflectance R_{NN} and emittance ε_N in a high-temperature air-oxidation process by the new spectrophotometer system shown in Section 2.2.

The specimen is heated by a heater /6/ attached on the back of the specimen, and the surface temperature is measured by a K-thermocouple of 100 μm in diameter welded on the surface. The surface temperature is scanned as follows. The surface is heated from room temperature up to 1100 K. Then the surface is kept at 1100 K for about 1 h. After that the surface is cooled in the ambient air.

This experiment represents the transition of radiation phenomena accompanied by the transition from an ideal surface in the laboratory to a real surface. A surface film is formed on the metal surface, and surface roughness is formed on the film surface. Corresponding to the change of the surface microstructure, interference and diffraction phenomena of radiation waves occur to change the spectra of reflectances, absorptance and emittance drastically.

3. Experimantal Results

3.1 Experimental results

Figures 4~7 show the experimental results of the spectra of hemispherical reflectance R_{NH}, specular reflectance R_{NN}, diffuse reflectance R_{ND}, absorptance A_N and emittance ε_N. Figures 4 and 5 show the spectrum transition of hemispherical reflectance R_{NH}, specular reflectance R_{NN} and diffuse reflectance R_{ND}, and spectrum transition of absorptance A_N and emittance ε_N, respectively. The axis λ is the wavelength of radiation in vacuum, and t is the time after the start of surface heating. Time t flows from the back to forward in these figures. Figures 6 and 7 show time transition of hemispherical reflectance R_{NH}, specular reflectance R_{NN}, diffuse reflectance R_{ND}, and time transition of absorptance A_N and emittance ε_N, respectively. Figures 6 and 7 show the same experimental data as those in Figures 4 and 5 as time transition of R_{NH}, R_{NN}, R_{ND}, A_N and ε_N at each wavelength. In Figures 6 and 7 the reflectances, absorptance and emittance are plotted in the logarithmic scale so that the absolute values can be read up to the significant figure of unity, and the figures are preferable for quantitative discussion. At the upper parts of the four-step figures values of shorter wavelengths are shown and at the lower parts values of longer wavelengths are shown. Of a number of curves in Figures 6 and 7 the curves which have the valleys or hills of the oscillation of interference in the left side correspond to the shorter wavelengths.

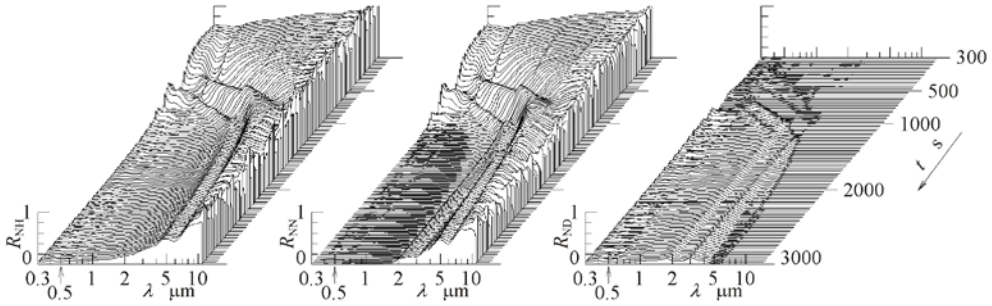

Figure 4. Spectrum transition of hemispherical reflectance R_{NH}, specular reflectance R_{NN} and diffuse reflectance R_{ND}.

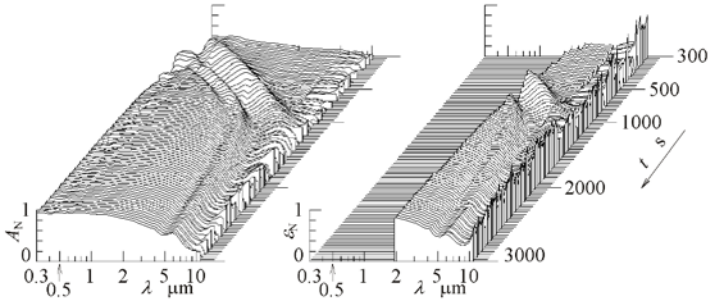

Figure 5. Spectrum transition of absorptance A_N and emittance ε_N.

3.2 Initial surface state

At the initial state of t=0 s the specimen surface is a clean optically smooth surface. The diffuse reflectance R_{ND} is zero over the spectral region of the present experiment. The hemispherical reflectance R_{NH} is equal to specular reflectance R_{NN}, and the specular reflectance R_{NN} is calculated by the spectra of optical constants of nickel[10]. With an increase of wavelength λ, specular reflectance R_{NN} increases monotonously and absorptance A_N (=1−R_{NH}) decreases monotonously.

3.3 Interference of radiation

When the surface is heated an oxide film is formed on the surface. In Figure 4, in the shorter wavelength side of the spectra of hemispherical reflectance R_{NH} and specular reflectance R_{NN}, a valley of the oscillation of radiation interference appears and secondly a hill appears. Correspondingly in Figure 5, in the shorter wavelength side of the spectrum of absorptance A_N, a hill of the oscillation of radiation interference appears and secondly a valley appears. With the growth of the surface film the valley and hill of the spectrum of hemispherical reflectance R_{NH} and specular reflectance R_{NN} shift to the longer wavelength side, and the hill and valley of the spectrum of absorptance A_N also shift to the longer wavelength side. Valleys and hills of the 2nd- and the 3rd-order interference appear in the shorter wavelength side and shift to the longer wavelength side. The spectrum of emittance ε_N is measured only in the longer wavelength region of 1.93≤λ≤10.9 μm by the present spectrophotometer system. In this spectral region a similar interference phenomenon is observed as that in the spectrum of absorptance A_N. These phenomena of interference is more clearly observed in the R_{NH}-t, R_{NN}-t, A_N-t and ε_N-t curves in Figures 6 and 7 where the values of R_{NH}, R_{NN}, A_N and ε_N are plotted in the logarithmic scale. The behavior of the interference in the shorter wavelength region of λ≤2 μm disappears after the 3rd-order interference appears.

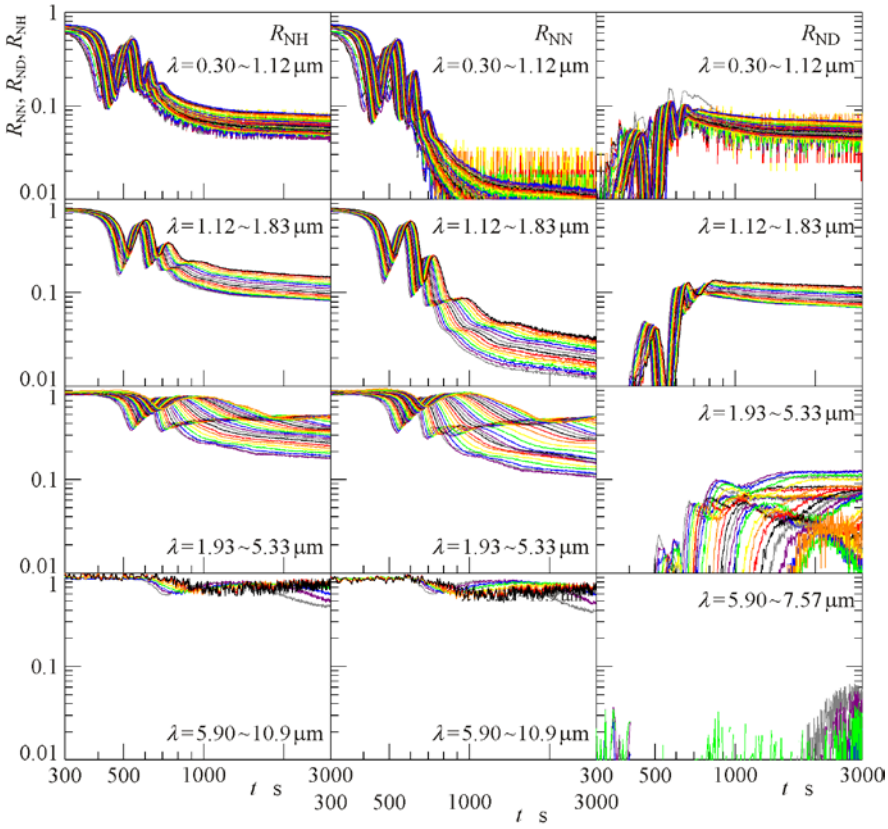

Figure 6. Time transition of hemispherical reflectance R_{NH}, specular reflectance R_{NN} and diffuse reflectance R_{ND}.

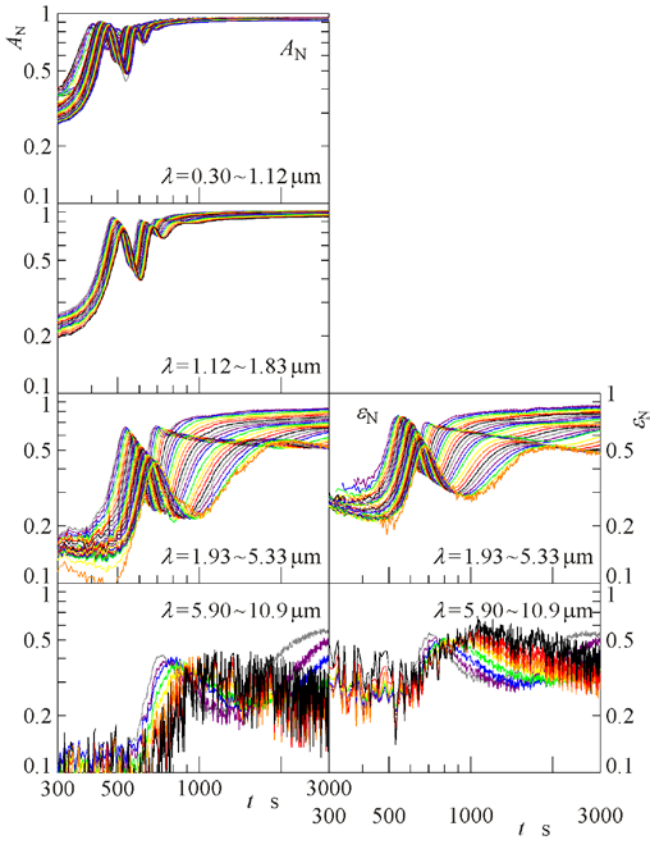

Figure 7. Time transition of absorptance A_N and emittance ε_N.

3.4 Diffuse reflection of radiation

On the surface of polycrystalline metal crystal grains of the surface film grow inhomogeneously and roughness appears on the film surface. Diffuse reflection occurs in the shorter wavelength side, and diffuse reflectance R_{ND}, which is zero initially, increases. This phenomenon extends gradually to the longer wavelength side. It is distinguished in Figure 4, and clearer quantitatively in Figure 6. In Figures 4 and 6 a clear behavior of radiation interference is found also in the spectra of diffuse reflectance R_{ND}. This phenomenon has been found first in the present experiment in which spectrum transition of diffuse reflectance R_{ND} could have been measured first.

By comparing the values of specular reflectance R_{NN} and diffuse reflectance R_{ND} in Figure 6, in the shorter wavelength region of $\lambda \leq 1.12$ μm specular reflectance R_{NN} is higher than diffuse reflectance R_{ND} at the initial stage of the film growth, but at the latter stage diffuse reflectance R_{ND} is higher than specular reflectance R_{NN}. In the longer wavelength region of $\lambda \geq 1.93$ μm specular reflectance R_{NN} is still higher even at the latter stage. In the shorter wavelength region diffuse reflectance R_{ND} increases with the film growth at the initial stage, but after that it decreases gradually. On these phenomena explanation is given in Section 4.3.

3.5 Absorption and emission of radiation

By neglecting the influence of spectrum oscillation of interference, absorptance A_N increases roughly with the growth of the surface film over the whole spectral region of the present experiment. This increase of absorptance A_N is remarkable particularly in the shorter wavelength region. Absorptance A_N in the visible region extends to an order of 95 % at the latter stage of the film growth. Most of the absorption is caused by the inherent absorption of the film material. In Figures 5 and 7 the interference behavior and absolute values of emittance ε_N are nearly the same as those of absorptance A_N. Figure 8 compares the values of absorptance A_N and emittance ε_N quantitatively, where the accuracy of the measurement of emittance ε_N is not so high as that for the absorptance A_N particularly in the longer infrared region. Considering this point it may be said that Kirchhoff's law $A_N=\varepsilon_N$ is validated again[7] at least in the wavelength region of $\lambda=2\sim7$ μm.

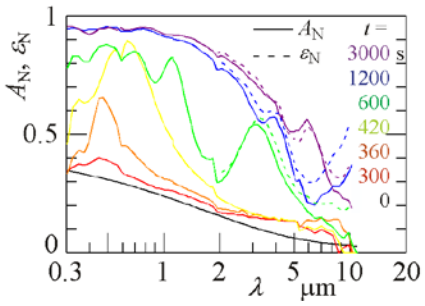

Figure 8. Spectrum transition of absorptance A_N and emittance ε_N.

4. Surface Phenomena and Radiation Phenomena

The present experiment deals with the transition of radiation characteristics accompanied by the transition of surface microstructure from an ideal surface in a clean laboratory to the real surface in the industrial environment representatively. The mechanism of the transition is characterized by the relation of average film thickness d, rms roughness σ of the film surface and wavelength of radiation λ. Since the wavelength region of the

present experiment is so wide, measured radiation phenomena seem to be complicated.

4.1 Surface roughness and diffuse reflection

Average film thickness d is evaluated approximately by,

$$d=\lambda_{(1)}/(4n) \tag{4}$$

where $\lambda_{(1)}$ is the wavelength of the valley of oscillation of the 1st-order interference in the measured spectra of specular reflectance R_{NN} and n is refractive index of the film. Refractive index n is of an order of 2 over the whole spectral region of the present experiment. Rms roughness σ of the film surface is known to grow to be 5~20 % of thickness d [4]. Accordingly, considering the behavior of specular reflectance R_{NN} in Figure 6 it is estimated that at t=700 s thickness d and roughness σ are of orders of 0.7 μm and 0.1 μm, respectively, and that at t=1200 s thickness d and roughness σ are of orders of 1.4 μm and 0.2 μm, respectively. The roughness σ measured by an optical microscope on the surface which was cooled down to room temperature after the experiment was of an order of 0.2 μm. Diffuse reflection becomes remarkable when the roughness σ increases to an order of 1 % of the wavelength λ of radiation considered. As observed in Figures 4 and 6 the diffuse reflection appears first in the shorter wavelength region and extends gradually to the longer wavelength region.

4.2 Interference in diffuse reflection

In Figure 6 the curves of time transition of diffuse reflectance R_{ND} and those of specular reflectance R_{NN} are compared. In the curves of diffuse reflectance R_{ND} in the shorter wavelength region of $\lambda \leq 1.12$ μm the valleys of the 1st-order interference is not observed since the values of the valleys are low, but successive hills of the 1st-order interference through hills of the 3rd-order interference are observed clearly. Paying attention to the curves of R_{NN} and R_{ND} at a wavelength λ, it is known that the valleys and/or hills of a curve of diffuse reflectance R_{ND} appear at a former time before they appear in the curve of specular reflectance R_{NN} when the surface film is thinner. For instance, in the second step figures from the top for diffuse reflectance R_{ND} and specular reflectance R_{NN} in Figure 6, the first hill of λ=1.83 μm (the rightmost curve) appears at t=500 s in the curve of diffuse reflectance R_{ND}, but it appears later at t=600 s in the curve of specular reflectance R_{NN}. Also, pay attention to the curves of R_{NN} and R_{ND} at a time t of the same film thickness d. For instance, see the second step figures for diffuse reflectance R_{ND} and specular reflectance R_{NN} in Figure 6. At t=600 s, in the curve of diffuse reflectance R_{ND} for λ=1.12 μm (the leftmost curve) the second hill of interference appears, and at the same time t=600 s, in the curve of specular reflectance R_{NN} for λ=1.83 μm (the rightmost curve) the first hill of interference appears. It suggests that the optical path in the film which characterizes the interference for diffuse reflectance R_{ND} is longer by about 1.2 (=2×1.12/(1×1.83)) times than that for specular reflectance R_{NN}. That is, the interference in diffuse reflectance R_{ND} is caused by the diffraction waves which travel a longer optical path obliquely as compared with those for specular reflectance R_{NN}.

4.3 Absorption, scattering and emission phenomena

By neglecting the influence of spectrum oscillation of interference, specular reflectance R_{NN} decreases monotonously with the film growth in the shorter wavelength region. Diffuse reflectance R_{ND} increases at the initial stage but decreases a little at the latter stage. Hemispherical reflectance R_{NH} decreases monotonously, absorptance A_N increases monotonously, and emittance ε_N increases monotonously. The factors characterizing such behaviors of the reflectances, absorptance and emittance are the following two: first,

absorption of radiation in the film, and second, scattering of radiation in the film surface. Both factors influence the phenomena stronger in the shorter wavelength region.

With the film growth and increase of thickness d, absorption of radiation which travels in the film increases. This absorption is caused by the film material. It decreases reflectances R_{NN}, R_{ND} and R_{NH} and increases absorptance A_N and emittance ε_N. On the other hand, with the film growth and increase of surface roughness σ scattering of radiation occurs on the film surface. The surface scattering decreases the specular reflection of radiation on the film surface and increases the diffuse reflection. At the same time, it causes multiple diffraction and interference of radiation on the surface, which decrease both of specular and diffuse reflection on the surface, and increase the absorption of the film-substrate surface system. The above two factors of absorption and scattering cause the phenomenon that diffuse reflectance R_{ND} once increases then turns to decrease.

4.4 Life of interference phenomena

In Figures 4~7 with the film growth the behavior of radiation interference once appears clearly in the shorter wavelength region of $\lambda \leq 5$ μm of the spectra of reflectances, absorptance and emittance, and then disappears. This phenomenon is also caused by radiation absorption in the film and radiation scattering on the film surface as described in Section 4.3. Both of absorption and scattering are strong in the shorter wavelength region. When the film grows thicker, the wave which travels in the film and returns to the film surface is absorbed stronger to be attenuated and it can not interfere with the wave reflected directly on the film surface with equivalent intensities. When the film grows optically thicker further, the wave once entered the film does not return to the surface to interfere with the directly reflected wave. Also, when the ratio (σ / λ) of the roughness of the film surface to the wavelength of radiation increases, the parallelness of the upper and lower interfaces of the film becomes worse and clear interference becomes difficult to occur. By the above two factors, clear interference in the shorter wavelength region could not have been observed in more than the 3rd-order interference in the case of the specular-finished nickel surface in the present experiment. At the longest wavelength λ=10.9 μm in the present experiment, influence of both absorption and scattering are weak and the interference behavior is clear even at the last time t=3000 s of the present experiment. The life of the interference generally depends strongly on the species of film materials, the size of polycrystals and the surface finish technique. In the spectra of specular reflectance R_{NN} of chromium whose surface was finished similarly the interference behavior has been observed up to the 6th-order interference even in the shorter wavelength region[8].

4.5 Performance of the developed spectrometer system

It has been demonstrated above that the spectrophotometer system developed in the present work clarifies the transition of the spectral quantities of reflection, absorption and emission as shown in Figure 1 entirely in the near-ultraviolet through infrared region. With respect to the experimental errors the previous paper[6] describes in detail. The error estimated in the measurements of reflectances and absorptance is of an order of ±0.3 % in the relative value at λ=0.70 μm, and ±1.0 % at λ=8.0 μm. The error estimated in the measurements of emittance ε_N of a surface at 1100 K is of an order of ±0.7 % in the relative value at λ=3.5 μm, and ±1.0 % at λ=8.0 μm. The error and the short wavelength limit of the measurement of emittance ε_N depend strongly on the surface temperature.

5. Conclusions

In the present work we have developed a spectrophotometer system for measuring

spectra of hemispherical reflectance R_{NH}, specular reflectance R_{NN}, diffuse reflectance R_{ND}, absorptance A_N and emittance ε_N of real surfaces in the spectral region of λ=0.30~10.9 μm simultaneously and repeatedly with a cycle time of 6 s. The system has been employed to measure the transition of the radiation spectra of a nickel surface in a high-temperature air-oxidation process to demonstrate the performance of the system. Obtained results are summarized as follows:

(1) It has been demonstrated that the developed spectrophotometer system measures transition of radiation phenomena of interference and diffraction in the wide spectral region from near-ultraviolet through infrared and clarifies radiation characteristics of real surfaces in thermal engineering entirely.

(2) It has been explained that transition of reflection, absorption and emission of radiation in the process of the change of surface microstructure from an ideal surface to a real surface seems to be complicated, but that the phenomena are caused by the change of the relation among the film thickness, surface roughness of the film, radiation absorption of the film and the wavelength of radiation.

(3) It has been clarified that the increase of radiation absorption of the film-substrate system with the film growth is caused not only by the increase of absorption in the film but also by the decrease of interface reflection due to the increase of scattering on the film surface.

(4) A clear interference phenomenon has been found in the diffusely reflected radiation. The interference is caused by radiation which travels a longer optical path in the surface film obliquely.

(5) Kirchhoff's law on the relation of absorptance A_N and emittance ε_N has been validated again.

Acknowledgement

This project has been partially supported by the Grant-in-Aid for Scientific Research ((A)20246039) of the Ministry of Education, Culture, Sports, Science and Technology, Japan. The authors have been accepted invaluable assistance from the co-researchers of the project, Professors K. Hanamura, Tokyo Institute of Technology, J. Yamada, Shibaura Institute of Technology, K. Miyazaki, Kyushu Institute of Technology and M. Matsumoto, Kyoto University.

References

(1) Makino, T., Thermal Radiation Spectroscopy for Heat Transfer Science and for Engineering Surface Diagnosis, *Heat Transfer 2002*, vol. 1, Taine, J. ed., (2002), pp. 55-66, Elsevier, Paris.

(2) Makino, T., Spectroscopic Approach to Thermal Radiation Science and Engineering of Solid Surfaces, *The 18th International Symposium on Transport Phenomena*, CD-ROM, (2007), pp. 136-145, no. Keynote 116.

(3) Wakabayashi, H. and Makino, T., A New Spectrophotometer System for Measuring Thermal Radiation Phenomena in a 0.30-11 μm Wavelength Region, *Measurement Science and Technology*, vol. 12, no. 12 (2001), pp. 2113-2120.

(4) Makino, T. and Wakabayashi, H., Thermal Radiation Spectroscopy Diagnosis for Temperature and Microstructure of Surfaces, *JSME International Journal*, ser. B, vol. 46, no. 11 (2003), pp. 500-509.

(5) Makino, T. and Wakabayashi, H., A Spectroscopic Approach for Controlling a

Spectrally Functional Thermal Radiation, *Proceedings of the 13th International Heat Transfer Conference*, CD-ROM, (2006), no. RAD-11.

(6) Makino, T. and Wakabayashi, H., Development of a Wide-Spectral-Range High-Speed Spectrophotometer System for Measuring Hemispherical Reflectance and Emittance of Surfaces Simultaneously, *Transactions of the JSME*, ser. B, vol. 75, no. 754 (2009), pp. 1329-1335.

(7) Makino, T. and Wakabayashi, H., Experimental Verification of Kirchhoff's Law on Thermal Radiation, *Transactions of the JSME*, ser. B, vol. 76, no. 769 (2010), pp. 1406-1411.

(8) Wakabayashi, H. and Makino, T., Thermal Radiation Phenomena of Surfaces of Chromium and Palladium in a High Temperature Environment, *Transactions of the JSME*, ser. B, vol. 76, no. 768 (2010), pp. 1258-1264.

(9) Siegel, R. and Howell, J. R., *Thermal Radiation Heat Transfer*, 3rd ed., (1992), pp. 47-91, Taylor & Francis, Bristol.

(10) Makino, T., Kawasaki, H. and Kunitomo, T., Study of the Radiative Properties of Heat Resisting Metals and Alloys (1st Report, Optical Constants and Emissivities of Nickel, Cobalt and Chromium), *Bulletin of the JSME*, vol. 25, no. 203 (1982), pp. 804-811.